Manuscript refereed by Dr Ken Mingard (NPL - National Physical Laboratory, United Kingdom)

Comparison Of Wear Performance Between Cemented Carbide, Ceramics And Wear Resistant Steels

Olivier Ther, Olivier Lavigne, Oscar Carrasco

Hyperion Materials & Technologies, Spain

Abstract

Cemented carbide materials are well known for their exceptional wear resistance and toughness combination, which make them an ideal choice for wear applications, particularly in mining industries. It is also well known, that for this family of materials, the wear resistance increases with the increase of the material's hardness. This paper compares the abrasion wear resistance, using the B611 test, of some cemented carbides with other material commonly used in wear applications, from high abrasion resistance steels to ceramics, such as alumina, zirconia, titanium carbide and silicon carbide grades. It is shown that by changing the material's type, the wear resistance is not only dependent of the hardness due to the different wear mechanisms encountered. Cemented carbide material shows outstanding performance in comparison with the other material.

Introduction

Cemented carbides are commonly used materials for wear application due to their exceptional mechanical performance (Gee and al., 2014). In mining processes, the abrasion wear of tools such as belt scrappers, conveyers or crushers is caused by the continuous handling of abrasive rock particles. The wear test ASTM B611 made for cemented carbides is of particular interest as it allows to simulate the abrasion wear mechanisms for different materials. The purpose of this paper is to compare cemented carbides with other family of materials (ceramics and steels) usually used in those applications and to understand the wear mechanisms and performances of those, in order to select the most appropriate material.

Materials & experimental protocol

Materials were obtained from the field (mining application) except the cemented carbide used for comparison.

The 10 analyzed materials could be separate in three families, ceramics (ZrO_2, ZTA, Al_2O_3-92; Al_2O_3-95, Al_2O_3-96, SiC), metal matrix composite, MMC, (TiC, cemented carbide ISOK20) and steels (Hardox 450, Hardox 500).

Samples were cut from the bulk of the different parts, mounted in bakelite resin, ground and polished down to 1 µm size diamond suspension for microstructural analysis, hardness and toughness measurements. Microstructural analyses were conducted with a ZEISS Supra55VP scanning electron microscope (SEM) equipped with energy dispersive X-ray spectroscopy (EDS) for elemental composition analysis. The composition of the different materials, determined through EDS analysis, are summarized in Table 1.

The cemented carbide used for comparison is a common submicron grade (WC grain size around 0.5 µm) with 10 wt.% Co. This cemented carbide (ISO K20) has a microstructure free of graphite or eta phase.

Table 1: Composition in wt.% of the studied material, * carbon content is not considered due to low content.

	Zr	Al	Y	O	Si	C	Ti	Fe	Ni	Mn	Cr	Mo	Hf	Ca
ZrO_2	70.1	0.1	4.5	23.5									1.8	
ZTA	14.7	39.4	1.1	44.4	0.4									
Al_2O_3-92		49.5		46.0	3.1									1.4
Al_2O_3-95		50.7		46.9	1.4									1.0

© European Powder Metallurgy Association (EPMA)

Table 2: continued.

	Zr	Al	Y	O	Si	C	Ti	Fe	Ni	Mn	Cr	Mo	Hf	Ca
Al_2O_3-96		52.2		45.6	1.2									1.0
SiC					74.3	25.4								
TiC					0.3	16.0	41.4	31.2	1.6	6.9		2.2		
Hardox 450 *					0.3			98.3		1.4				
Hardox 500 *					0.3			98.2		0.7	0.6			

Vickers hardness and fracture toughness measurements were carried out in accordance with ISO 28079:2009 for cemented carbides. Three indentations per material were made at 30 kgf using a Vickers Limited equipment. The indent diagonals and the crack lengths emerging form the indentation corners were measured with a light optical microscope at a magnification of 500x. The same methodology was used for the different material in order to allow a comparison between them.

Table 3: Vickers hardness and Palmqvist toughness obtained for the different material, * indentation induces a spalling of the material, ** indentation done at 30 kgf does not generate cracks long enough to perform the measurement.

	ZrO_2	ZTA	Al_2O_3-92	Al_2O_3-95	Al_2O_3-96	SiC	TiC	Hardox 450	Hardox 500	K20
HV30	1160	1230	1030	1205	1265	2040 *	845	455	505	1600
K_{1C} (MPa $m^{0.5}$)	9.0	5.4	6.1	5.6	6.4	n/a *	n/a **	n/a **	n/a **	10.5

The abrasive wear resistance of the materials was determined by following the ASTM B611 standard. Brown alumina sand (FEPA grit F30) was used as the abrasive particles. Samples cut from the bulk of the different parts were of rectangular shape (40 x 20 x 5 mm^3) with a ground surface finish (220 grit). The wear volume of the material, W expressed in mm^3, is presented and defined as W=L/d, where d is the material density in g/cm^3 and L the weight loss in g. The density was measured using Archimedes' principle (ASTM B311-93).

Table 4: Measured density and measured wear volume obtained from ASTM B611 test.

	ZrO_2	ZTA	Al_2O_3-92	Al_2O_3-95	Al_2O_3-96	SiC	TiC	Hardox 450	Hardox 500	K20
d (g/cm^3)	5.99	4.09	3.62	3.71	3.73	3.02	6.06	7.81	7.80	14.46
W (mm^3)	114	425	770	294	277	303	290	133	120	21

Results & Discussion

Figure 1 shows the abrasion volume loss of the various materials considered in this work plotted in function of their hardness, together with data obtained from the literature (Gee, et al., 2005) for a range of WC–Co hardmetals tested in the same experimental conditions.

© European Powder Metallurgy Association (EPMA)

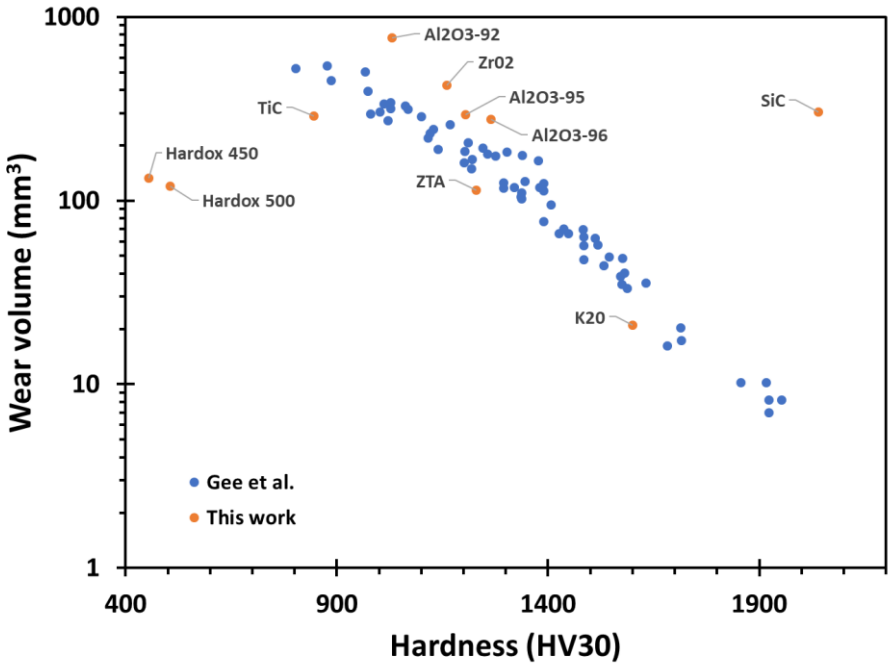


Figure 1: Relationship between abrasion volume loss and hardness for range of WC–Co hardmetals for ASTM B611 Alumina (Gee, and al, 2005) and comparison with results obtained in this work.

Wear analysis

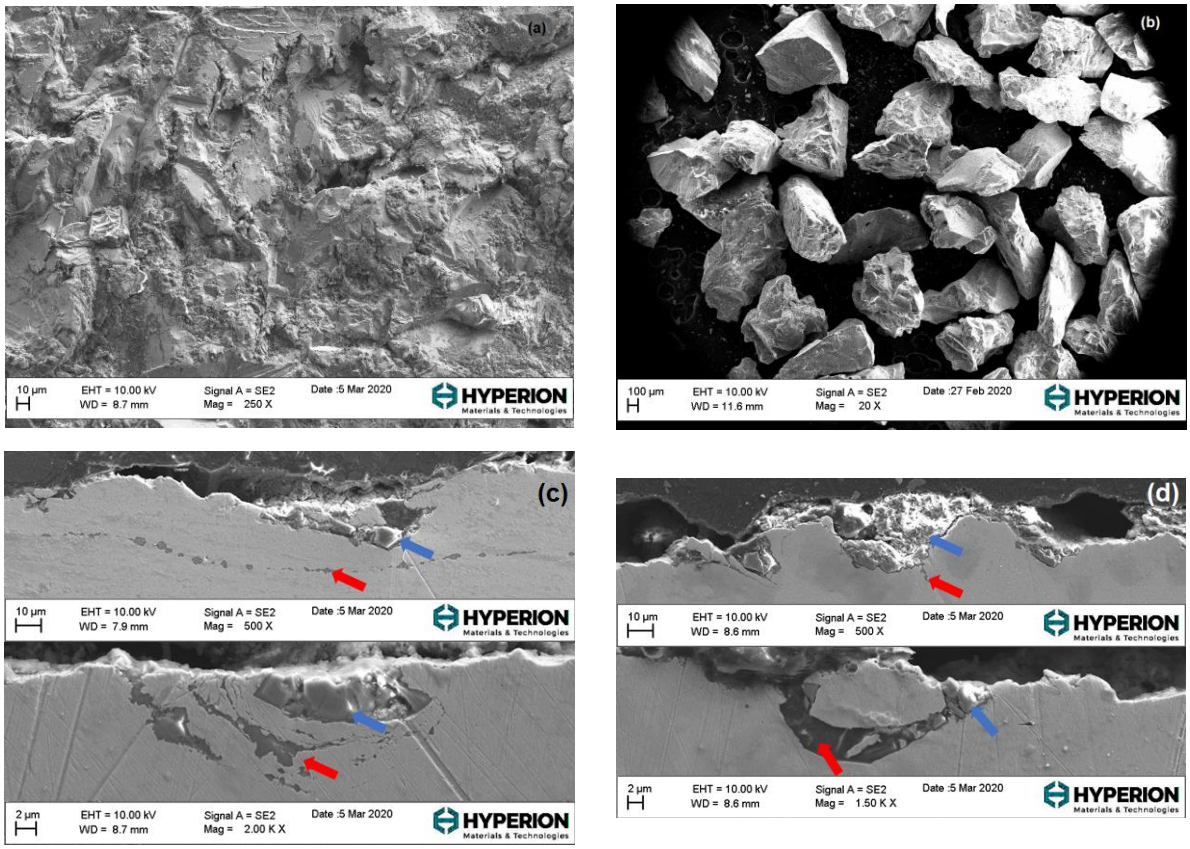


Figure 2 : Wear track of Hardox 450 after B611 testing (a), sand particle used for testing (b), cross sections of the wear track Hardox 450 (c, top and bottom), and cross sections of the wear track Hardox 500 (d, top and bottom).

© European Powder Metallurgy Association (EPMA)

The two steel materials Hardox 450 and 500 showed high deformation and rock penetration (Fig.2). Deformations observed in the wear track correspond to the shape of the sand particles. Sand and debris act like an indenter (blue arrows) and the presence of cracks (filled with bakelite, red arrows) can be observed. The rock penetration tends to rip-off the surface of the material.

Wear of cemented carbide has been extensively studied. Engqvist (Engqvist, 2000) showed that the wear is dependent of the hardness of abrasive particles. In case of hard abrasives (defined as 1.2 times the hardness of the given cemented carbide) the material is removed by plastic deformation and by cracking of the WC grains. When the abrasive is considerate as soft, the main wear mechanism is the extrusion of binder and subsequent removal of WC grains (Beste, 2004).

In the present case, K20 material, the wear looks quite uniform and smooth. The cross section inside the wear track shows that the first layer of WC (in contact with the sand) is deformed and that the binder phase below has been pushed out (Figure 3a). Additionally, in the wear track, Figure 3b shows plastic deformation (slip bands) of WC grains (red arrows) and cracked WC grains (purple arrow), pull out of WC grains (blue arrow) and re-embedment of fractured WC grains in the binder phase (green arrow). This is in good agreement with the available literature (Gee and al., 2014).

The observation of all those mechanisms is in good agreement with the previous observations as the hardness of brown alumina sand is reported to be between 1800-2200HV which is around the 1.2 threshold ratio. This could explain why all reported mechanisms are observed.

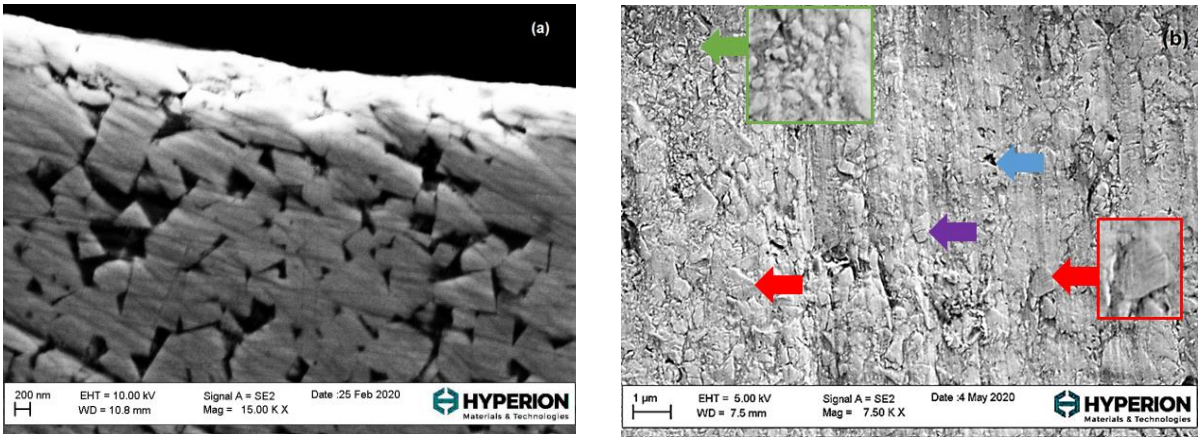


Figure 3: Cross section inside the wear track (a) and wear track of K20 material (b).

For the SiC material, the cross section inside the wear track (Figure 4a) shows the initial cracks propagation (red arrow) leading to the spalling of a large portion of material (blue arrow). This is due to the low toughness of this material and explains its poor wear behavior despite its high hardness. Pictures taken in the wear track (Figure 4b) confirm this observation by showing wear caused by material breakage.

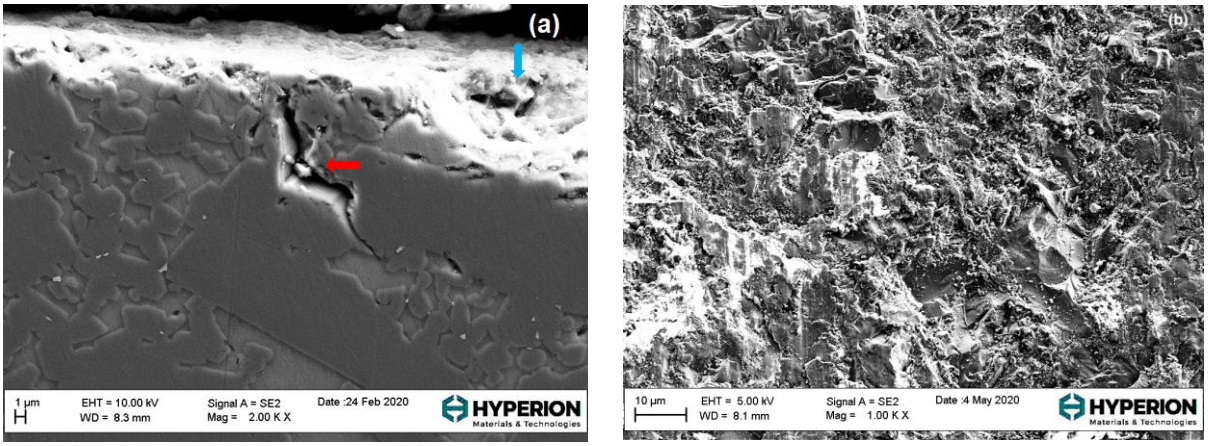


Figure 4: Cross section inside the wear track (a) and wear track of SiC material (b)

The wear of TiC material looks quite smooth. The observation of the wear track cross section shows cracks parallel to the surface corresponding to a layer of high plastic deformation (Figure 5a). The

© European Powder Metallurgy Association (EPMA)

wear track seems to confirm this observation by showing highly plastic deformed areas and pull-out of material (Figure 5b).

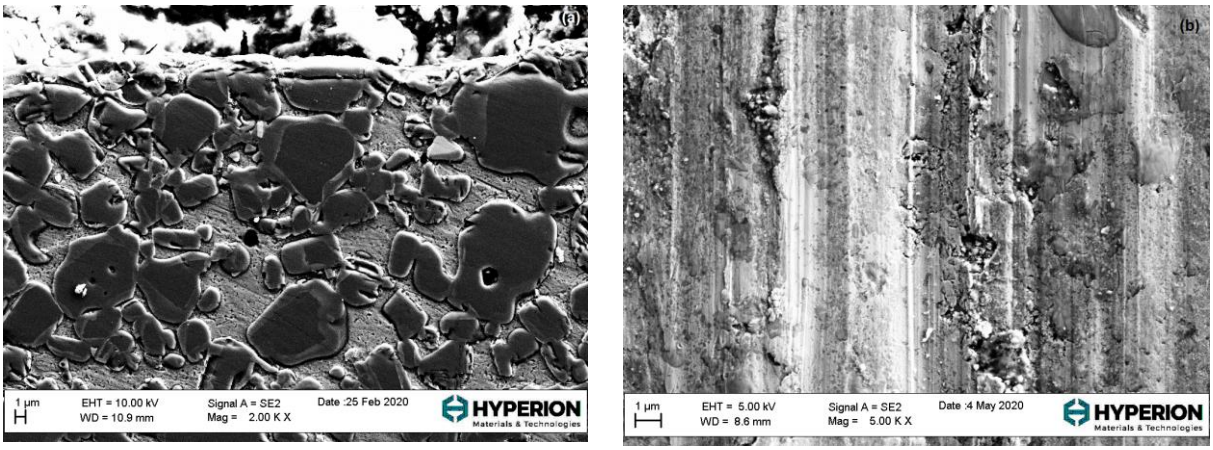


Figure 5: Cross section inside the wear track (a) and wear track of TiC material (b).

The observation of the wear track of ZTA material shows pull-out and large fractured grains (Figure 6b). Cross section's observations show grains pull-out (Figure 6a).

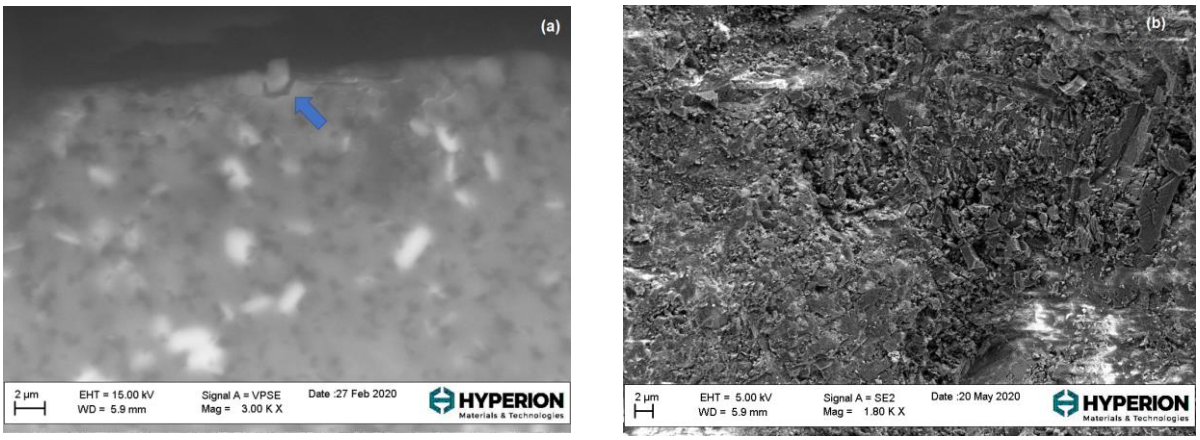


Figure 6: Cross section inside the wear track (a) and wear track of ZTA material (b).

The wear of zirconia material seems to be related to a mechanism of subsurface cracking parallel to the surface followed by delamination (Figure 7a and 7b). This is in good agreement with Conoci's observation on 3Y-TZP after pin on disk tests (Conoci and al., 1999).

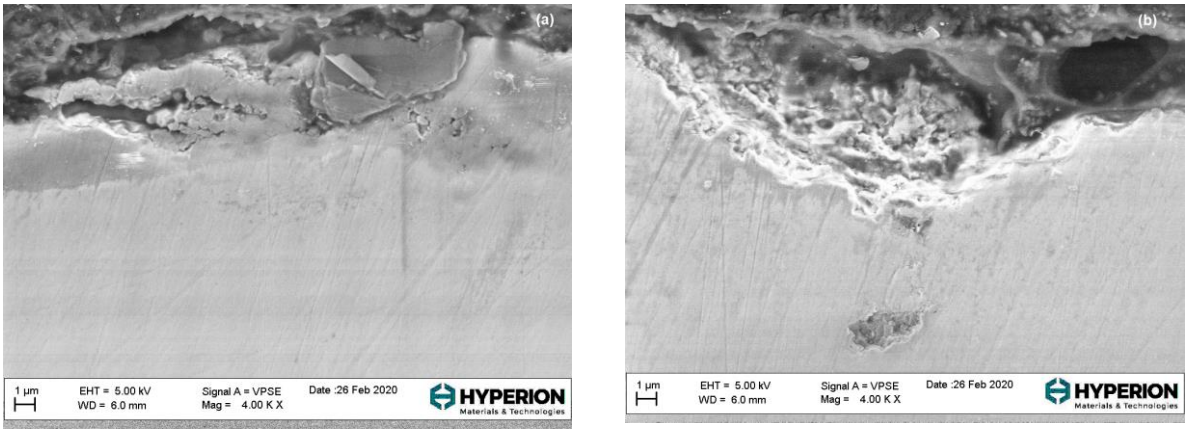


Figure 7: Cross section inside the wear track of Zirconia material.

The observation inside the wear tracks seems also to indicate some plastic deformation of the zirconia material prior to delamination (Fig.8).

© European Powder Metallurgy Association (EPMA)

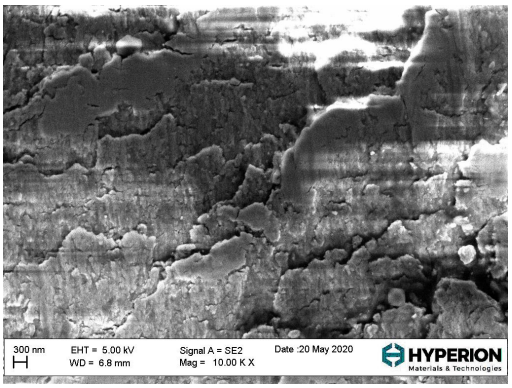


Figure 8: Zirconia inside the wear track

With Al_2O_3, the wear looks similar for all three different alumina materials. For the Al_2O_3-95 sample a high quantity of fractured grains is visible in the cross section (Figure 9d).

The wear track indicates a breakage inside alumina grains and then pull out (Figure 9a, 9b and 9c). Some plastic deformations of alumina grain seem more present in the Al_2O_3-92 (Figure 9a).

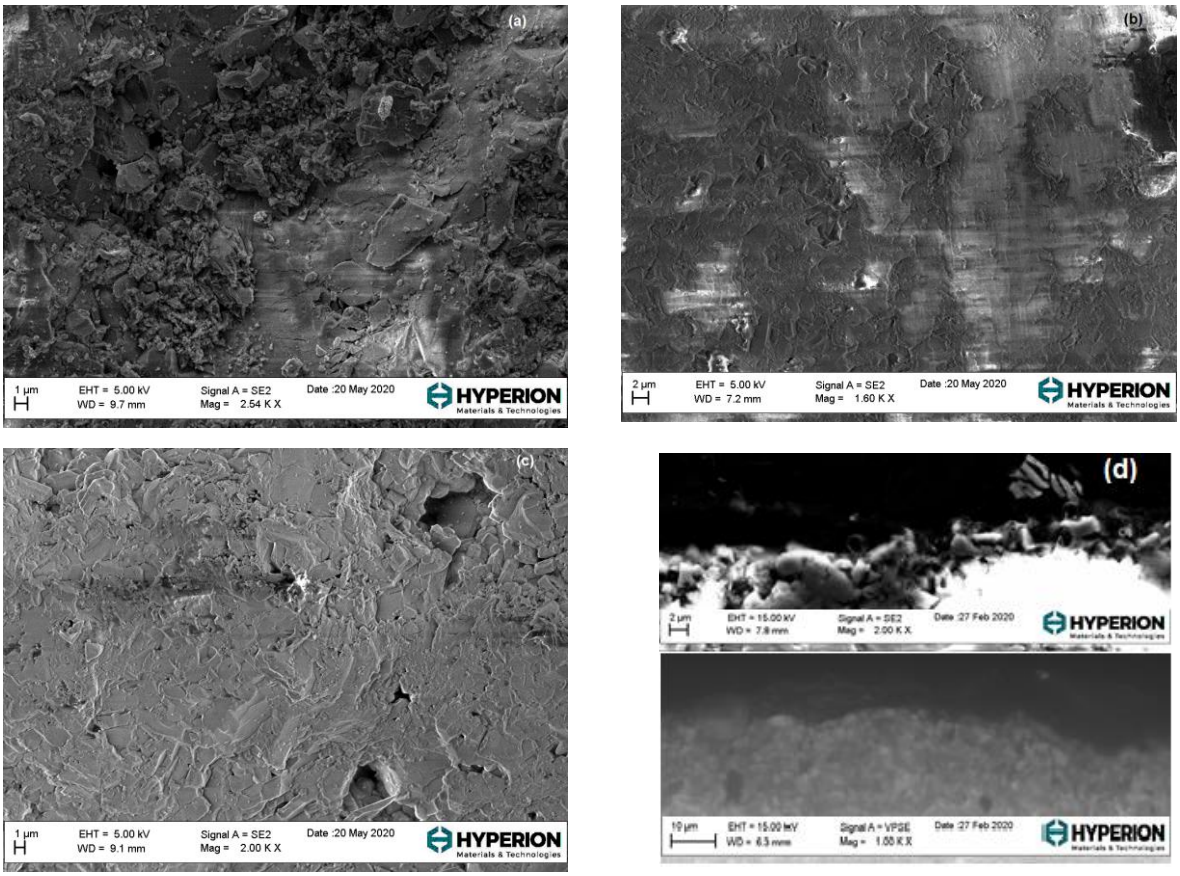


Figure 9: Wear track of Al_2O_3 material Al_2O_3-92 (a), Al_2O_3-95 (b), Al_2O_3-96 (c) and cross section of the wear track of Al_2O_3-92 (d, top) and Al_2O_3-95 (d, bottom).

Conclusion

The wear behavior of ceramics with a hardness up to 1300HV30 follows quite well the trend of cemented carbides. For higher hardness, the performance of ceramics is degraded due to their insufficient toughness.

Cemented carbides above 1300HV30 show better performance than other materials due to their combination of high hardness and toughness.

© European Powder Metallurgy Association (EPMA)

The SiC material despite its very high hardness does not perform well due to its extremely low toughness. In real conditions, this material is expected to perform even worse, as these conditions imply some degradation mechanisms by impact.

Hardox 450 and 500 perform very well for their level of hardness, but in real conditions their performances could be limited by corrosion mechanisms.

References

ASTM B611 – 85 (2005). *Abrasive Wear Resistance of Cemented Carbides***.**

Beste, U. 2004. *On the nature of cemented carbide wear in rock drilling., Doctoral thesis.* Uppsala : Uppsala University, 2004.

Engqvist, H. 2000. *Microstructural Aspects on Wear of Cemented Carbides, Doctoral thesis.* Uppsala : Uppsala University, 2000.

Gee, M.G., Gant, A.J. and Mingard, K.P. 2014. *Comprehensive hard materials, 1.12 - Wear of Hardmetals.* 2014. pp. 363-383.

Gee, M.G., Roebuck, B. and Gant, A.J. 2005. *Abrasive wear testing with the ASTM B611 and modified ASTM G65 rotating wheel test systems .* Reutte, Austria : 16th Int. Plansee Seminar high performance PM materials, 2005. pp. 1235–1249. Vol. 2, 30 May–3 June 2005 .

Conoci, S., Melandri, C. and De Portu, G. 1999. *Wear of 3Y-TZP containing compressive residual stresses at the surface.* : Journal of Materials Science, 1999, Vol. 34, pp. 1009–1015.

© European Powder Metallurgy Association (EPMA)